Dynamics of sulfur adlayer transformations at metal/electrolyte interfaces

G. Andreasen, C. Vericat, M. E. Vela, and R. C. Salvarezza

Citation: J. Chem. Phys. **111**, 9457 (1999); doi: 10.1063/1.480331
View online: http://dx.doi.org/10.1063/1.480331
View Table of Contents: http://jcp.aip.org/resource/1/JCPSA6/v111/i21
Published by the American Institute of Physics.

COMMUNICATIONS

Dynamics of sulfur adlayer transformations at metal/electrolyte interfaces

G. Andreasen, C. Vericat, M. E. Vela, and R. C. Salvarezza[a)]
Instituto de Investigaciones Fisicoquímicas Teóricas y Aplicadas (INIFTA), Sucursal 4, Casilla de Correo 16, 1900 La Plata, Argentina

(Received 4 June 1999; accepted 21 September 1999)

The dynamics of adsorbed sulfur on Au(111) at the metal/electrolyte interface has been followed by scanning tunneling microscopy. The increase in the negative surface charge density induces the transformation from rectangular S_8 to a $\sqrt{3}\times\sqrt{3}$ *R*30° lattice. This process involves desorption of sulfur atoms as HS^- ions, formation of rectangular tetramer intermediates, and displacement of atoms from the intermediate to nearest hollow sites. A further increase in the negative charge density produces desorption of the $\sqrt{3}\times\sqrt{3}$ *R*30° lattice from terraces. Sulfur atoms remain strongly bonded to step edges. Experimental data provide an estimation of the excess of binding energy close to step edges. Correlation between S and thiol adlayer desorption data has been found. © *1999 American Institute of Physics.* [S0021-9606(99)71445-5]

The understanding of the dynamics of adsorbed atoms and molecules on solid surfaces is a complex and fascinating problem that can be elucidated by using local probes such as scanning tunneling microscopy (STM) and atomic force microscopy. These studies require high quality real-time imaging at the atomic and molecular level and dynamic processes taking place at a relatively slow rate.[1] In contrast to structural STM data there are few examples of dynamical studies at the atomic and molecular level.

Sulfur-containing molecules adsorbed on metals are good candidates to study adsorbate dynamics. Recent *in situ* STM studies have shown the richness and complexity of the dynamics of adsorbed alcanethiol layers on Au(111).[2,3] In electrolyte solutions structural transformations at the substrate and at adsorbed layers can be induced by slight changes in the surface charge density at the metal/electrolyte interface resulting from small changes in the applied potential (E). Therefore, the dynamics of these transformations can be studied under clean and well-controlled experimental conditions.[4] Reconstruction of low index gold surfaces[5] and the order/disorder transitions at adsorbate domains[6] are examples of dynamical processes induced by E that can be followed by *in situ* STM.

In this paper we report *in situ* STM imaging data of the transformations induced by changes in E that take place in S layers adsorbed on Au(111). S adsorption on metals has attracted considerable interest because S is a poison for heterogeneous catalytic reactions,[7] hinders metal passivity by competing with oxygen species,[8] and promotes metal embrittlement by the enhancement of hydrogen absorption.[9] Previous *in situ* STM data on the adsorption of sulfur layers on Au(111) have shown that a $\sqrt{3}\times\sqrt{3}$ *R*30° lattice[10,11] is initially formed, followed by the formation of rectangular S_8 species as the applied potential E is increased positively.[10] Our results reveal that the transformation from the rectangular S_8 to the $\sqrt{3}\times\sqrt{3}$ *R*30° lattice is reversible and occurs in a narrow potential region. This involves adsorption/desorption of S species, the formation of rectangular tetramer intermediates, and finally the rearrangement of these intermediates by displacement of S atoms to the neighbor hollow sites. A further increase in the negative surface charge density at the metal electrolyte/interface induces fast S desorption from Au(111) terraces as HS^- ions, while S atoms remain adsorbed at step edges. The excess of binding energy of S atoms at these sites with respect to terraces is 0.4 eV. Correlation between the reductive desorption of S as HS^- and dodecanethiol adlayers is also presented.

Electrochemical runs and *in situ* STM imaging were made using a Nanoscope III electrochemical STM (Digital Instruments Inc.). Additional electrochemical measurements were made in a conventional glass-made electrochemical cell. Au films evaporated on glass (250 nm thick onto Robax glass, AF Berliner Glas KG, Germany) with a 2-nm-thick chromium undercoating were used as substrate. As observed by STM, these films exhibit atomically smooth (111) terraces separated by monoatomic high steps. A large area Au counterelectrode and a Pd/H_2 reference electrode were used. Potentials in the text are referred to the saturated calomel electrode (SCE). Apiezon covered Pt–Ir tips were used for STM imaging. The electrolyte solution was 0.1 M NaOH $+3\times10^{-3}$ M Na_2S prepared from high purity chemicals. STM images were taken in the constant current mode using set point currents 10/20 nA and bias voltages 0.3 V/0.6 V.

A typical current density (j)/E profile (Fig. 1) recorded for Au(111) in the working solution shows for $E < -1.20$ V a net negative current density associated with the hydrogen evolution reaction (HER), two humps at -1.13 V (AI) and -1.17 V (CI), and then two well-defined peaks at -0.90 V (AII) and -0.95 V (CII). While the origin of the humps is unknown, peaks AII/CII have been assigned to the

a)Electronic mail: robsalva@inifta.unlp.edu.ar

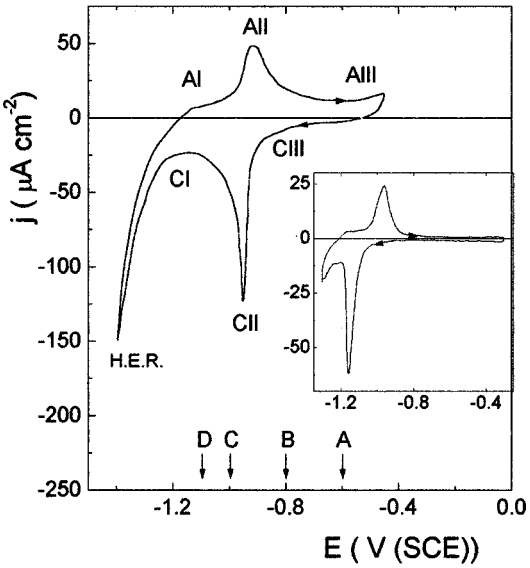

FIG. 1. Typical j vs E profile for Au(111) recorded at a scan rate $v = 0.05\ \mathrm{V\ s^{-1}}$ in 0.1 M NaOH+3×10^{-3} M Na_2S. Labels *A, B, C* and *D* (arrows) indicate E values for STM imaging. The direction of the potential scan is indicated on the j/E profile. The inset shows the j vs E profile obtained for the desorption (negative potential scan) of a dodecanethiol SAM on Au(111) and subsequent readsorption (positive potential scan) at the same v in 0.1 M NaOH.

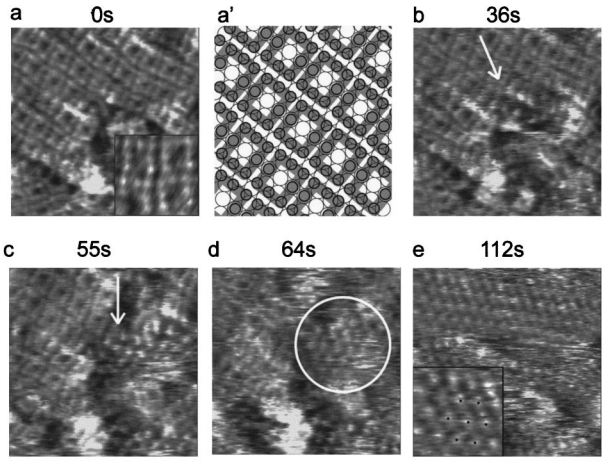

FIG. 2. Sequential STM images ($7.3\times7.3\ \mathrm{nm^2}$, raw data) of the Au(111) surface in 0.1 M NaOH+3×10^{-3} M Na_2S at different E values and times. (a) $E=-0.6$ V, the inset at the lower right-hand corner shows rectangles where individual S atoms are clearly distinguished; (a′) scheme showing the rectangular S_8 species (in gray) on Au(111). Open and gray circles stand for Au atoms and S atoms, respectively. (b)–(e) $E=-0.8$ V. The dynamics of the $S_8 \Rightarrow \sqrt{3}\times\sqrt{3}\ R30°$ S lattice transformation is shown. The arrow in (c) indicates the appearance of the first hexagon. The circle in (d) indicates a $\sqrt{3}\times\sqrt{3}\ R30°$ S lattice domain growing around the first hexagon. The inset in (e) shows a detail of the hexagonal $\sqrt{3}\times\sqrt{3}\ R30°$ S lattice. Black dots indicate a typical hexagon of the $\sqrt{3}\times\sqrt{3}\ R30°$ S lattice with $d=0.5$ nm.

adsorption/desorption of the $\sqrt{3}\times\sqrt{3}\ R30°$ S lattice on Au(111)[10] according to the reaction:

$$HS^- + Au(111) = S-Au + H^+ + 2e. \quad (1)$$

The charge density involved in this process is $q_{II}=150\pm10\ \mu\mathrm{C\ cm^{-2}}$, which for the number of atoms in the $\sqrt{3}\times\sqrt{3}\ R30°$ lattice implies a charge transfer of two electrons per S atom. At more positive potentials (AIII), the positive current density increases due to the formation of polymeric S species.[10] The latter are reduced at the hump CIII (−0.80 V). Note that the current related to HER is enhanced after S adsorption. The arrows in Fig. 1 indicate the E values at which STM images were taken.

The *in situ* $7.3\times7.3\ \mathrm{nm^2}$ STM image [Fig. 2(a)], taken at $E=-0.6$ V (*A*, in Fig. 1), shows $0.62\pm0.03\times0.57\pm0.03\ \mathrm{nm^2}$ quasirectangular patterns separated by ≈0.3 nm. The rectangles, which exhibit a certain degree of disorder, are distributed on three adjacent terraces. Eight atoms with nearest-neighbor distances of $d\approx0.31$ nm in the direction of the long edge and $d\approx0.29$ nm in the direction of the short edge are observed in most of the rectangles [inset in Fig. 2(a)]. These data suggest that S_8 species are a polymeric form of adsorbed S, although the values of d are greater than those reported for polysulphide species ($d=0.20-0.22$ nm).[12] Therefore, values in the range $0.29\ \mathrm{nm}<d<0.31\ \mathrm{nm}$ for the S–S distance in S_8 should result from a balance between S–Au and S–S interactions. A scheme consistent with the STM images for the rectangular S_8 species on Au(111) is shown in Fig. 2(a′). This configuration maximizes the number of S atoms in hollow sites. Displacements of S atoms to ''wrong'' hollows sites introduce the disorder shown in some rectangles and explain the error bars in the rectangle size measurements. Note that bulk S_8 ring structures involve a boatlike conformation; therefore the planar S_8 structure reveals a strong adsorbate–substrate interaction.[10,13] When E is changed from −0.6 to −0.8 V (*B*, in Fig. 1) the sequential STM images [Figs. 2(b)–2(e)] show the progressive transformation of the rectangular patterns into the $\sqrt{3}\times\sqrt{3}\ R30°$ lattice with $d=0.5$ nm. The process, involving 112 s, results in desorption as HS^- ions of about $\frac{1}{2}$ of the total S atoms from the rectangles, as can be estimated from a detailed analysis of Figs. 2(a) and 2(e). Details about how the structural transformation proceeds can be envisaged from the sequential STM images. After changing E from −0.60 to −0.80 V, the STM image shows that two S_8 were transformed into rectangular-shaped tetramers [arrow in Fig. 2(b)]. Immediately afterwards a hexagon [the arrow in Fig. 2(c)], corresponding to the $\sqrt{3}\times\sqrt{3}\ R30°$, is formed with two of the S atoms which were vertices of a near tetramer. After a few seconds a domain of the $\sqrt{3}\times\sqrt{3}\ R30°$ lattice [the circle in Fig. 2(d)] grows around the initial hexagon. Therefore, the initial step is desorption of the four S atoms in the central positions of the rectangular S_8 structure, resulting in a tetramer. The reason for the formation of tetramers is that the S–S distance is close to 0.5 nm, and only small displacements of the remaining S atoms to the neighbor hollow sites are needed to form the $\sqrt{3}\times\sqrt{3}\ R30°$ lattice [Fig. 2(e)]. The steps involved in the transformation from S_8 to $\sqrt{3}\times\sqrt{3}\ R30°$ lattice are schematically shown in Fig. 3. Note that this process takes place at hump CIII (Fig. 1). When E is changed back to $E=-0.60$ V, the $\sqrt{3}\times\sqrt{3}\ R30°$ lattice is transformed into the S_8 rectangular species, i.e., the process is reversible. Note that the noise in the STM images is related to desorption and movement of atoms during the electrochemical reaction, as the image quality is largely improved when the reaction is completed.

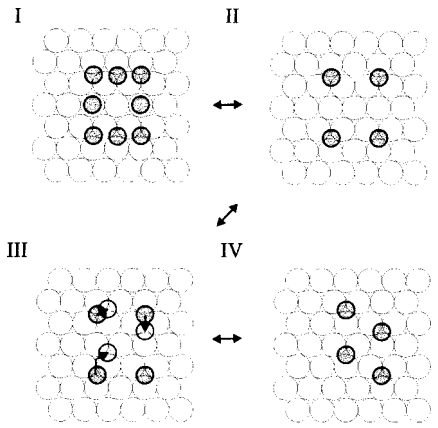

FIG. 3. Schemes showing the $S_8 \Rightarrow \sqrt{3}\times\sqrt{3}\ R30°$ S lattice transformation. (I) S_8; (II) tetramer formation after desorption of S atoms; (III) displacements of S atoms to nearest hollow sites; (IV) S atoms forming the $\sqrt{3}\times\sqrt{3}\ R30°$ primitive unit cell. Small gray and large open circles indicate S and Au atoms respectively. In III small open circles indicate the final positions toward which S atoms move to form the $\sqrt{3}\times\sqrt{3}\ R30°$ lattice.

After changing E from -0.80 to -1.0 V (C, in Fig. 1) the $\sqrt{3}\times\sqrt{3}\ R30°$ lattice is rapidly removed from the terraces leaving the (1×1) Au (111) lattice ($d=0.29$ nm) [Fig. 4(a)]. Electrochemical data show that this process is completed in 0.5 s so that it is impossible to follow this process in real time. Sulfur atoms still remain adsorbed at step edges due to the increased coordination number at these sites. In Fig. 4(a) three rows of S atoms adsorbed at step edges are observed. Although the rows exhibit a certain degree of disorder, we found S–S distances of 0.5–0.6 nm along the row, and ≈0.4 nm between rows, S–S distances being compatible with hollow sites in the Au(111) lattice. The third row of S atoms is not complete because the excess of binding energy decreases from the n to $n+1$ row. In fact, when E is decreased to $E=-1.1$ V (D, in Fig. 1) the third row is easily removed [Fig. 4(b)]. Complete desorption of the first and second rows [Fig. 4(c)] is more difficult as it requires $E=-1.17$ V. In these images the absence of atomic resolution at the bare Au(111) terraces can be related to the HER, which proceeds at a non-negligible rate in this potential range. The S desorption from step edges as HS^- (hump CI in Fig. 1) takes place simultaneously with HER, which appears enhanced after S adsorption (Fig. 1). The $\sqrt{3}\times\sqrt{3}\ R30°$ desorption from terraces is a reversible process: when E is changed from -1.0 to -0.80 V S readsorption at terraces takes place leading again to the $\sqrt{3}\times\sqrt{3}\ R30°$ lattice.

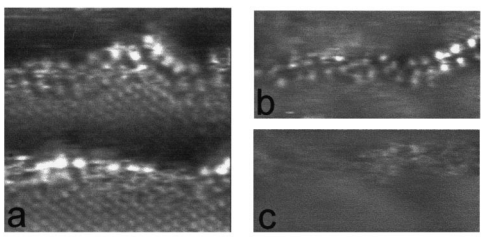

FIG. 4. STM images of the Au(111) surface in 0.1 M NaOH+3×10^{-3} M Na_2S. (a) (7.3×7.3 nm^2, raw data) After changing E from -0.8 to -1.0 V. The Au(111) lattice and three rows of S atoms adsorbed at step edges are clearly seen. (b) (7.3×3.47 nm^2, raw data) After changing E from -1.0 to -1.1 V. The third row of S atoms has been removed. (c) (7.3×3.47 nm^2, raw data) Image taken at $E=-1.17$ V showing complete S desorption.

Our STM results demonstrate that peak CII corresponds to S desorption from Au(111) terraces as HS^-, while S desorption from step edges takes place at -1.17 V. From the potential difference between peak CII and -1.17 V, and considering two electrons per S atom in reaction[1] we can estimate an excess of binding energy close to step edges of ≈0.4 eV, i.e., 12% of the S–Au(111) binding energy.[14] A similar result has been reported for the adsorption of Xe on Pt.[15] Although humps AI/CI could be due to S adsorption/desorption on/from terraces of the minority (110) and (100) orientations the potential range of these humps suggests that they were related to S adsorption/desorption at/from step edges.

Results for S adlayer transformations are important to understand the complex reductive desorption of self-assembled monolayers (SAM) of thiols on Au(111).[16] Thiols on Au(111) form $\sqrt{3}\times\sqrt{3}\ R30°$ lattices and superlattices. Comparison of XPS data shows almost no difference in the binding energies of S atoms and S heads of thiol molecules adsorbed on Au(111),[17] although the formation of S–S bounds for the $c(4\times2)$ thiol superlattice has been suggested.[18] We have made *in situ* STM and electrochemical runs for a dodecanethiol SAM on Au(111) prepared by immersion in ethanolic solutions containing 0.05 mM dodecanethiol for 24 h. The dodecanethiol-covered Au(111) surface was then immersed in 0.1 M NaOH. At $E=-0.6$ V the same $\sqrt{3}\times\sqrt{3}\ R30°$ lattice found for S is observed, without evidences of S_8 formation, i.e., contamination of the thiol adlayer with S is negligible.[17] When the potential is scanned in the negative direction up to -1.3 V, the $\sqrt{3}\times\sqrt{3}\ R30°$ lattice is removed at a current peak similar to CII (Fig. 1 inset) but located 0.2 V more negative and involving $\frac{1}{2}q_{II}$. This value indicates one electron transfer for desorption of a thiol molecule from the $\sqrt{3}\times\sqrt{3}\ R30°$ lattice rather than the two electron transfer found for S desorption as SH^- ions. The negative potential shift of the peak observed for thiol-covered Au with respect to CII could arise from the hydrophobicity of the hydrocarbon chains, and to a minor extent from van der Waals interactions among hydrocarbon chains. These contributions make desorption of the $\sqrt{3}\times\sqrt{3}\ R30°$ lattice more difficult for thiols than for adsorbed S. It has been suggested that hydrophobic forces are much stronger and long-range than van der Waals attractions at small separations.[19] In fact, the potential shift of about 0.2 V for dodecanethiol desorption could be explained by considering one electron transfer and hydrophobic forces of about 0.023 eV/CH_2.[19]

The fact that even for S on Au(111) the shortest S–S distances found are ≈0.3 nm (S_8) suggests that disulfide bonds ($d=0.20-0.22$ nm)[18] cannot be formed in thiol adsorbed monolayers at least at 298 K.[20]

In summary we have followed the dynamics of $S_8 \Leftrightarrow \sqrt{3}\times\sqrt{3}\ R30°$ lattice transformation in real time. This process occurs through desorption, formation of adsorbed intermediate species, and adatom displacement. The adsorbed intermediate has a geometry that allows atoms to reach the final structure by small low-energy displacements. In this

case the reversible transformation results from a balance between the S–S and the S–Au interaction energies, which depend on the surface charge density at the substrate/electrolyte interface. By increasing the negative surface charge density the fast desorption of the $\sqrt{3}\times\sqrt{3}$ $R30°$ lattice takes place leaving bare Au and S atoms at step edges. The large excess of binding energy at step edges could explain the effect of S as a poison in heterogeneous catalytic reactions. The adsorption/desorption of a SAM of thiols on Au(111) resembles the adsorption/desorption of the $\sqrt{3}\times\sqrt{3}$ $R30°$ S adlayer, the main differences being the one electron transfer and the hydrophobicity of hydrocarbon chains.

The authors thank Agencia Nacional de Promoción Científica y Tecnológica PICT No. 97-1993 and CONICET (PIP 0897) (Argentina) for the financial support of this work.

[1] B. Borovski, M. Krueger, and E. Ganz, Phys. Rev. Lett. **78**, 4229 (1997); R.-L. Lo, I.-S. Hwang, M.-S. Ho, and T. T. Tsong, *ibid.* **80**, 5584 (1998).
[2] G. E. Poirier and D. Pylant, Science **272**, 1145 (1996); G. E. Poirier, Langmuir **15**, 1167 (1999).
[3] F. Terán, M. E. Vela, R. C. Salvarezza, and A. J. Arvia, J. Chem. Phys. **109**, 5703 (1998).
[4] H. Roher, in *Nanoscale Probes of the Solid Liquid Interface*, edited by A. A. Gewirth and H. Siegenthaler, NATO ASI Series Vol. 288 (Kluwer, Dordrecht, 1995), p. 1; O. M. Magnussen, J. Hotlos, R. J. Nichols, D. M. Kolb, and R. Behm, Phys. Rev. Lett. **64**, 2929 (1990).
[5] X. Gao, A. Hamelin, and M. J. Weaver, Phys. Rev. Lett. **67**, 618 (1991).
[6] F. Cunha and N. J. Tao, Phys. Rev. Lett. **75**, 2376 (1995).
[7] C. H. Bartholomew, P. K. Agrawal, and J. R. Katzer, Adv. Catal. **31**, 135 (1982).
[8] J. Oudar and P. Marcus, Appl. Surf. Sci. **3**, 48 (1979); P. Marcus, *Advances in Localized Corrosion*, edited by H. S. Isaacs, U. Bartocci, and S. Smialowska (NACE, 1990), p. 289.
[9] *Adsorption on Metal Surfaces*, edited by J. Benard (Elsevier, Amsterdam, 1983).
[10] X. Gao, Y. Zhang, and M. J. Weaver, J. Phys. Chem. **96**, 4156 (1992).
[11] R. L. McCarley, Y.-T. Kim, and A. J. Bard, J. Phys. Chem. **97**, 211 (1993).
[12] B. Meyer, Chem. Rev. **76**, 367 (1976).
[13] T. E. Lister and J. L. Stickney, J. Phys. Chem. **100**, 19568 (1996).
[14] H. Sellers, Surf. Sci. **294**, 99 (1993).
[15] V. Marsico, M. Blanc, K. Kuhnke, and K. Kern, Phys. Rev. Lett. **78**, 94 (1997).
[16] D. E. Weisshaar, B. D. Lamp, and M. D. Porter, J. Am. Chem. Soc. **114**, 5860 (1992); M. M. Walczak, C. A. Alves, B. D. Lamp, and M. D. Porter, J. Electroanal. Chem. **396**, 103 (1995).
[17] C.-J. Zhong, R. C. Brush, J. Anderegg, and M. D. Porter, Langmuir **15**, 518 (1999).
[18] P. Fenter, A. Eberhardt, and P. Eisenberger, Science **266**, 1216 (1994).
[19] J. N. Israelachvili, in *Intermolecular and Surface Forces* (Academic, London, 1994), pp. 353, 408; D. W. Hatchett, R. H. Uibel, K. J. Stevenson, J. M. Harris, and H. S. White, J. Am. Chem. Soc. **120**, 1062 (1998).
[20] G. J. Kluth, C. Carraro, and R. Maboudian, Phys. Rev. B **59**, R10449 (1999).